Journal of Sound and Vibration (2003) **259**(3), 724–732
doi:10.1006/jsvi.2002.5225, available online at http://www.idealibrary.com on IDEAL®

EXPLANATION OF FREQUENCY CROSS OVERS AND CORRESPONDING MODE SHAPE CHANGES IN THE FREE VIBRATION PROBLEM OF CLAMPED CYLINDRICAL PANELS

B. Sivasubramonian

Launch Vehicle Design Group, Vikram Sarabhai Space Centre, Thriruvananthapuram 695 002, *India*

AND

A. M. Kulkarni and G. Venkateswara Rao

Structural Engineering Group, Vikram Sarabhai Space Centre, Thriruvananthapuram 695 002, *India*

(*Received* 3 *December* 2001, *and in final form* 25 *April* 2002)

1. INTRODUCTION

Thin panels are used in aircrafts, launch vehicles, etc. as structural members. These panels are supported on all sides at the edges. As the region where the panel is supported is additionally stiffened, it can be assumed that the boundary conditions at the edges are closer to that of a clamped condition. In the present paper the free vibration behavior of clamped panels are studied for different curvatures to identify the frequency cross overs and mode shape changes through the associated strain energies (i.e., membrane, bending and shear).

Finite element, analytical and experimental methods are extensively used for the free vibration analysis of plate and shell problems. Bogner *et al.* [1] formulated a 48-degrees-of-freedom shell element having continuity of the first derivatives along the different elements sharing the same boundary. Olson and Lindberg [2] developed a 28-degrees-of-freedom shell element which gave frequencies for a cantilever curved panel even with a 4×4 mesh within 10% of the experimentally obtained values for the first 12 modes. Leissa [3] carried out extensive compilation of data available on the free vibration of shells. Free vibration characteristics of singly curved rectangular plates were obtained by extended Rayleigh Ritz (ERR), finite element and Kantorovich methods by Petyt [4], where non-dimensional frequency parameters with aspect ratio, thickness and curvature were studied. For simply supported conditions, exact solutions were obtained in this study. For studying clamped edges, various approximate methods were used and results obtained were compared with the experimental data and the EER method is recommended. Cheung and Cheung [5] studied the free vibration of cylindrical panels by integral equation technique for the effects of variation of radius, thickness and the Poisson ratio. Blevins [6] found out the frequency characteristics of shallow cylindrical curved panels. Srinivasan and Bobby [7] studied the vibrations of a circular cylindrical panel using the integral equation technique by varying the curvature and thickness for all the edges, clamped condition. Lee *et al.* [8] studied the free vibration of cantilver shells of rectangular plan form using the shallow and deep shell theories by the Ritz method for a wide range of shell parameters.

0022-460X/02/$35.00

Generally, it is observed that when the radius reduces for a given size of the panel the frequency crossovers and the corresponding mode shape changes do exist. The present study attempts to explain this phenomena through the associated membrane, bending and shear strain energies using a finite element formulation.

2. FINITE ELEMENT FORMULATION

The four noded 28-degrees-of-freedom (each node having 7 degree of freedom, namely, w, w_x, w_y, u, u_y, v and v_y, where, subscript denotes partial derivative with respect to that variable) cylindrical shell element of rectangular planform, developed using the displacement approach by Olson and Lindberg [2], has been used in the present study. The element co-ordinate system is shown in Figure 1.

The displacement polynomials used in the finite element formulation are

$$w(x,y) = a_1 + a_2x + a_3y + a_4xy + a_5x^2 + a_6y^2 + a_7x^2y + a_8xy^2 + a_9x^3 + a_{10}y^3 + a_{11}x^3y + a_{12}xy^3, \quad (1)$$

$$u(x,y) = a_{13} + a_{14}x + a_{15}y + a_{16}xy + a_{17}y^2 + a_{18}xy^2 + a_{19}y^3 + a_{20}xy^3, \quad (2)$$

$$v(x,y) = a_{21} + a_{22}x + a_{23}y + a_{24}xy + a_{25}y^2 + a_{26}xy^2 + a_{27}y^3 + a_{28}xy^3. \quad (3)$$

The strain–displacement relations for the cylindrical panel are

$$\begin{aligned} \varepsilon_{xx} &= \frac{\partial u}{\partial x}, \quad \varepsilon_{yy}\frac{\partial v}{\partial y} + \frac{w}{R}, \\ \varepsilon_{xy} &= \frac{\partial u}{\partial y} + \frac{\partial v}{\partial x}, \quad \kappa_{xx} = -\frac{\partial^2 w}{\partial x^2}, \\ \kappa_{yy} &= -\frac{\partial^2 w}{\partial y^2} + \frac{1}{R}\frac{\partial v}{\partial y}, \quad \kappa_{xy} = \frac{1}{R}\frac{\partial v}{\partial x} - 2\frac{\partial^2 w}{\partial x \partial y}. \end{aligned} \quad (4)$$

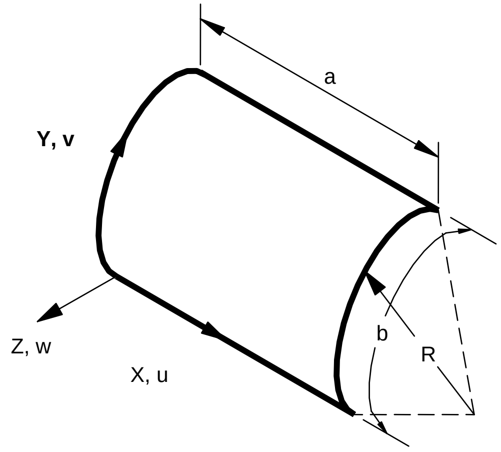

Figure 1. Co-ordinate system of the cylindrical shell element.

The strain energy U of the element is given by

$$U = \frac{1}{2}\iint \left\{ \begin{array}{c} C\left[\varepsilon_{xx}^2 + \varepsilon_{yy}^2 + 2\upsilon\varepsilon_{xx}\varepsilon_{yy} + \dfrac{1-\upsilon}{2}\varepsilon_{xy}^2\right] \\ +D\left[\kappa_{xx}^2 + \kappa_{yy}^2 + 2\upsilon\kappa_{xx}\kappa_{yy} + \dfrac{1-\upsilon}{2}\kappa_{xy}^2\right] \end{array} \right\} \mathrm{d}x\,\mathrm{d}y, \tag{5}$$

where

$$C = \frac{Et}{(1-\upsilon^2)} \quad \text{and} \quad D = \frac{Et^3}{12(1-\upsilon^2)}. \tag{6}$$

The expression for the kinetic energy T of the element is

$$T = \frac{1}{2}\rho t \iint \left(\dot{u}^2 + \dot{v}^2 + \dot{w}^2\right) \mathrm{d}x\,\mathrm{d}y. \tag{7}$$

Using the above expressions the elemental stiffness matrix $[k]$, further subdivided as $[k_m]$, $[k_b]$ and $[k_s]$ as explained below and the elemental mass matrix $[m]$ are generated.

Using the following expressions extracted from equation (5), sub-stiffness matrices $[k_m]$, $[k_b]$ and $[k_s]$ for membrane, bending and shear stiffnesses, respectively, are computed from

$$U_m = \frac{1}{2}\iint C\left(\varepsilon_{xx}^2 + \varepsilon_{yy}^2 + 2\upsilon\varepsilon_{xx}\varepsilon_{yy}\right) \mathrm{d}x\,\mathrm{d}y, \tag{8}$$

$$U_b = \frac{1}{2}\iint D\left(\kappa_{xx}^2 + \kappa_{yy}^2 + 2\upsilon\kappa_{xx}\kappa_{yy}\right) \mathrm{d}x\,\mathrm{d}y, \tag{9}$$

$$U_s = \frac{1}{2}\frac{1-\upsilon}{2}\iint (C\varepsilon_{xy}^2 + D\kappa_{xy}^2)\, \mathrm{d}x\,\mathrm{d}y. \tag{10}$$

After assembling the elemental matrices, the matrix eigenvalue problem governing the vibration of the panel can be written as

$$[[K_m] + [K_b] + [K_s]]\{\delta\} - \omega^2[M]\{\delta\} = \{0\}. \tag{11}$$

Equation (14) can be solved for the eigenfrequencies and the eigenvectors by using any standard algorithm to extract the eigenvalues and the eigenvectors. To evaluate the strain energy break up namely membrane, bending and shear for each mode the following expressions are used:

$$\tfrac{1}{2}[\delta]^{\mathrm{T}}[K_m][\delta] = \textit{diagonal}\ [SE_m], \tag{12}$$

$$\tfrac{1}{2}[\delta]^{\mathrm{T}}[K_b][\delta] = \textit{diagonal}\ [SE_b], \tag{13}$$

$$\tfrac{1}{2}[\delta]^{\mathrm{T}}[K_s][\delta] = \textit{diagonal}\ [SE_s], \tag{14}$$

where, the 'i'th diagonal term represents the energies for the 'i'th mode.

From Equations (12) to (14) the energy break up for each mode for the membrane, bending and shear energies of a vibrating panel can be evaluated, as percentage of the total strain energy $[SE_T]$ given by

$$[SE_T]\tfrac{1}{2}\{\delta\}^{\mathrm{T}}[K]\{\delta\}, \tag{15}$$

where

$$[K] = [[K_m] + [K_b] + [K_s]]. \tag{16}$$

3. NUMERICAL RESULTS AND DISCUSSIONS

The first five frequencies and percentages of the membrane, bending and shear strain energies of a 500 mm × 500 mm × 2 mm thick panel made of steel ($E = 21{,}000\ \mathrm{Kg/mm^2}$, $\rho = 7{\cdot}8\mathrm{E}{-}10\ \mathrm{kg\ s^2\,m^{-3}}$ and $\nu = 0{\cdot}3$) are obtained for different curvatures. A 20 × 20 finite element mesh for the present problem has been found to give converged results within 1% accuracy [9]. Panels with different R/t values ranging from 10 000 to 500 have been considered in the present study. Figure 2 gives the variation of the frequencies for the first five modes, with varying R/t. Figures 3–7 give the energy variation of membrane, bending and shear energies as percentages of the total strain energy in the panel for different R/t values for the first five modes. The corresponding mode shapes in terms of '*m*' and '*n*' are given for the some representative values of R/t in Table 1.

It is seen that as R/t increases, the panel behaves similar to that of a plate, which it should be, and the panel frequencies are high for low R/t values because of the curvature effect. For mode 1 (Figure 3), the mode change is seen at R/t of around 700 and around 2400 and the corresponding energy percentage changes can be seen in the plots, as the membrane, bending and shear energy. Mode shape changes from (1,2) to (1,3) for R/t of around 700 and (1,1) to (1,2) for R/t of around 2400. It can be seen that when R/t decreases the bending energy reduces and the membrane energy increases. The mode shape change is due to the change in the energy level at R/t of around 2400. Similar mode shape change and the associated energy changes can be seen at R/t of around 700 also.

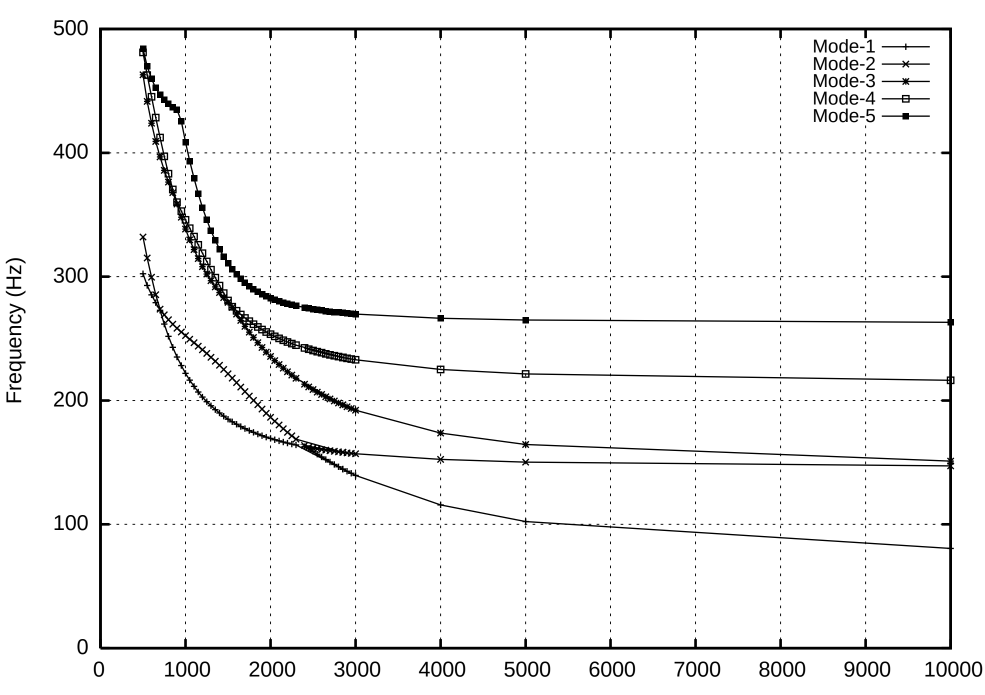

Figure 2. Frequencies of a square clamped panel.

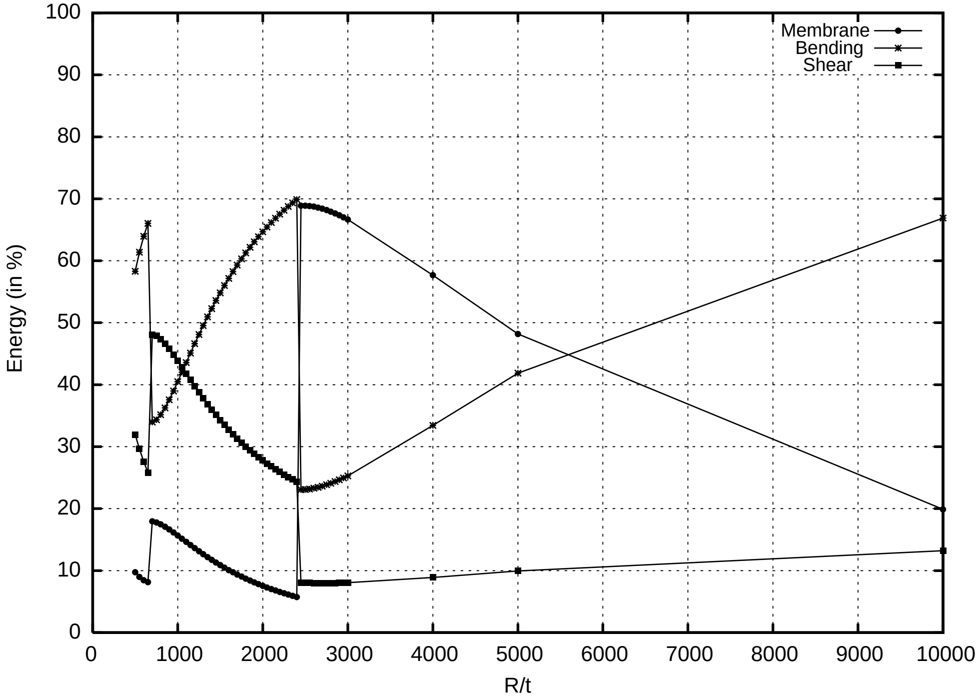

Figure 3. Various energies for mode 1 for square clamped panel.

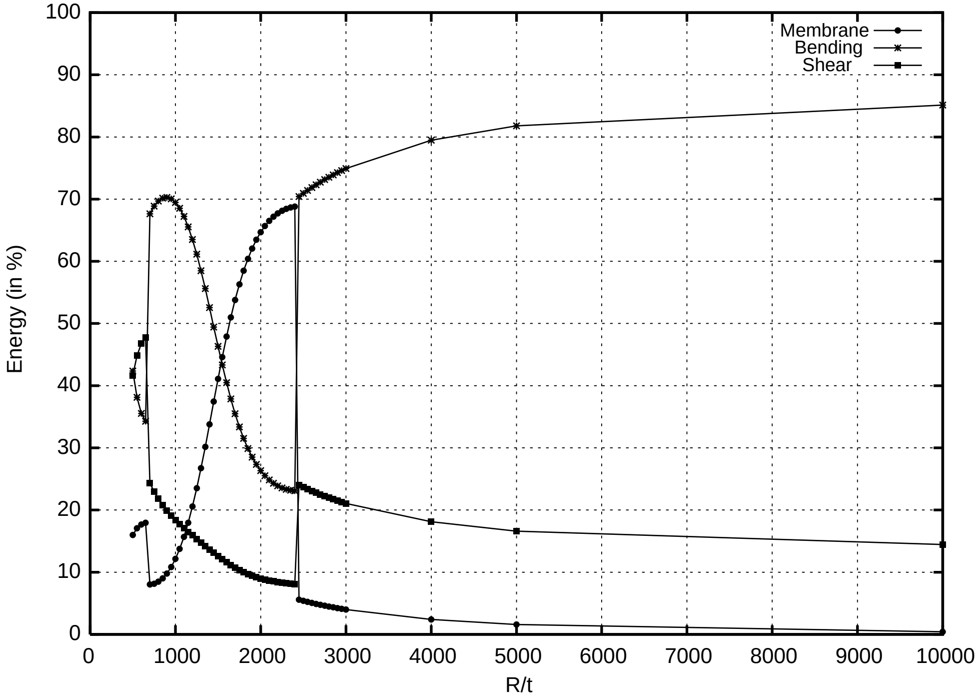

Figure 4. Various energies for mode 2 for square clamped panel.

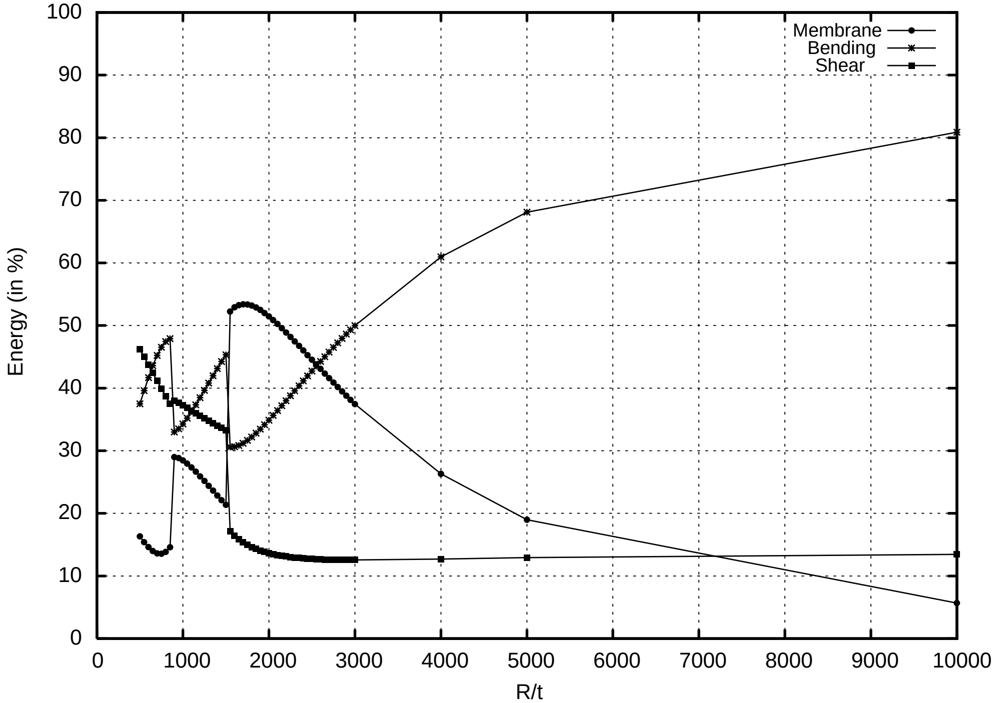

Figure 5. Various energies for mode 3 for square clamped panel.

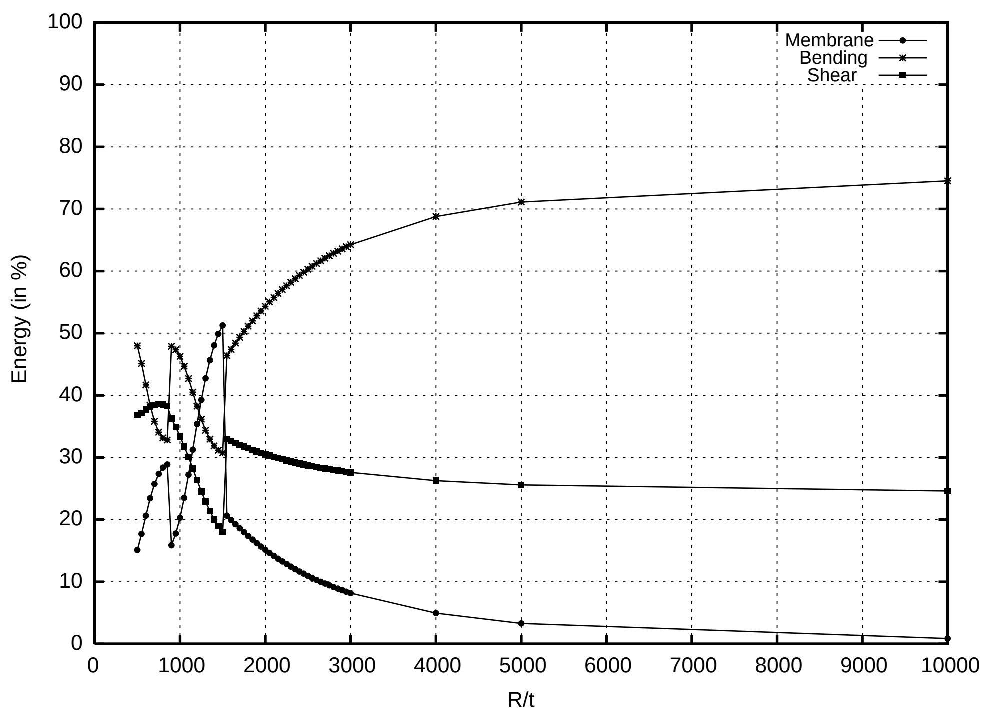

Figure 6. Various energies for mode 6 for square clamped panel.

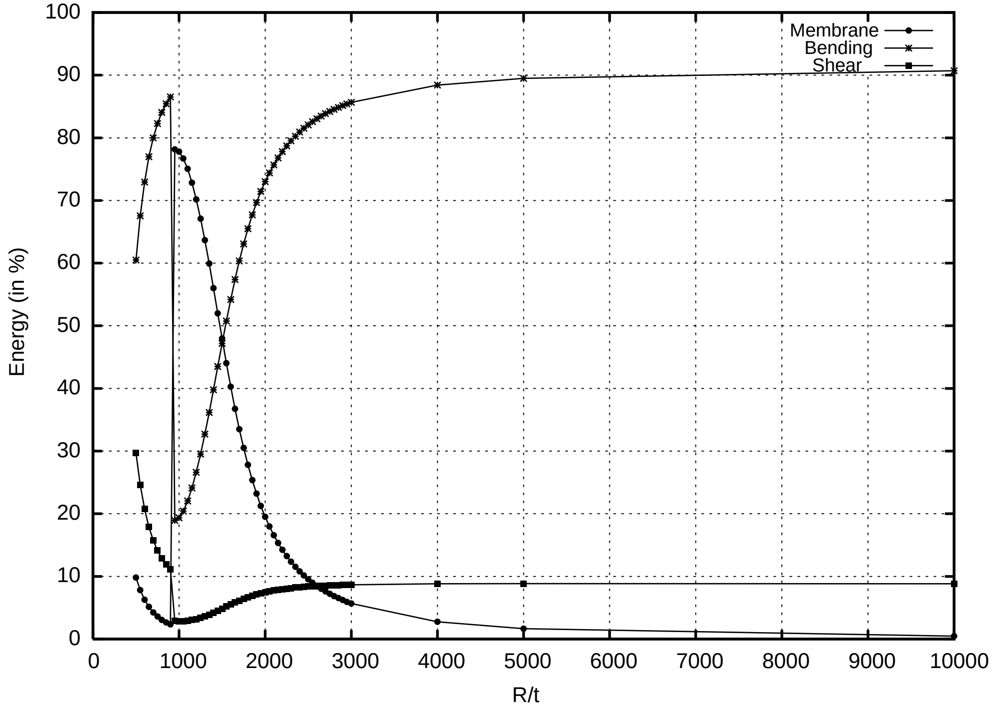

Figure 7. Various energies for mode 7 for square clamped panel.

TABLE 1

Mode shapes (m, n) for different R/t

R/t	500	750	1000	2000	3000	4000	10 000
Mode 1	1,3	1,2	1,2	1,2	1,1	1,1	1,1
Mode 2	1,4	1,3	1,3	1,3	2,1	2,1	2,1
Mode 3	2,3	2,3	2,2	1,2	1,2	1,2	1,2
Mode 4	2,4	2,4	2,3	2,2	2,2	2,2	2,2
Mode 5	1,4	1,4	1,3	1,3	1,3	1,3	1,3

For mode 2 (Figure 4), the mode shape changes at the same R/t as that of mode 1. The difference seems to be that while bending and shear energy changes dictate the mode shape change at R/t of around 2400, it is the bending and shear energy combination, which causes mode shape change at R/t of around 700. The corresponding mode changes are (1,3) to (1,4) for R/t of around 700 and (2,1) to (1,3) for R/t of around 2400.

Modes 3 (Figure 5) and 4 (Figure 6) have mode shape changes at R/t of around 900 and around 1500. While for modes 3 and 4 all the energy levels dictate the mode shape change for R/t of around 1500, it is the membrane and bending energy that is causing the mode shape change at R/t of around 900. The mode shape changes are (2,3) to (2,4) for R/t of around 900 and (2,2) to (2,3) for R/t of around 1500.

Mode shape change for the fifth mode (Figure 7) is found to occur at R/t of around 900 where there is a sudden change in the membrane and bending energies and the mode shape change is from (1,3) to (1,4).

4. CONCLUSIONS

The frequencies and associated mode shapes of circular panels clamped on all sides are studied by the finite element method. The mode wise strain energies, namely, the membrane, bending and shear energies are computed as percentages of the total strain energy. First five frequencies, mode shapes and the corresponding strain energies are computed for different curvatures. Based on the energy changes, it is possible to explain the frequency cross overs and the mode shape changes of the vibrating panel.

REFERENCES

1. F. Bogner, R. L. Fox and L. A. Schmidt 1967 *American Institute of Aeronautics and Astronautics Journal* **5**, 745–750, A cylindrical shell discrete element.
2. M. D. Olson and G. M. Lindberg 1972 *NRC-NAE-LR*-497. A finite cylindrical shell element and the vibrations of a curved fan blade.
3. Leissa A. W. 1973 *NASA-SP*-288. Vibration of shells.
4. M. Petyt 1971 *Journal of Sound and Vibration* **15**, 381–395. Vibration of curved plates.
5. Y. K. Cheung and M. S. Cheung 1972 *Journal of Sound and Vibration* **22**, 59–73. Vibration analysis of cylindrical panels.
6. R. D. Blevins 1981 *Journal of Sound and Vibration* **75**, 145–149. Natural frequencies of shallow cylindrical curved panels.
7. R. S. Srinivasan and W. Bobby 1976 *Journal of Sound and Vibration* **46**, 43–49. Free vibration analysis of non circular cylindrical shell panels.
8. J. K. Lee, A.W. Leissa and A. J. Wang 1982 *International Journal of Mechanical sciences* **25**, 361–383. Vibration of cantilevered circular cylindrical shells; Shallow versus deep shell theory.
9. B. Sivasubramonian, A. M. Kulkarni, G, Vekateswara Rao and A. Krishnan 1997 *Journal of Sound and Vibration* **200**, 227–234. Free vibration of curved panels with cutouts.

APPENDIX A: NOMENCLATURE

a,b	length and width of the panel
E	Young's modulus.
t	panel thickness
$[k]$	elemental stiffness matrix
$[k_m]$, $[k_b]$, $[k_s]$	elemental membrane, bending and shear stiffness matrices respectively.
$[K]$	global stiffness matrix
$[K_m]$, $[K_b]$, $[K_s]$	global membrane, bending and shear stiffness matrices respectively.
m,n	longitudinal and circumferential wave number
$[m]$	elemental mass matrix
$[M]$	global mass matrix
R	radius of the panel
$[SE_m]$, $[SE_b]$, $[SE_s]$	membrane, bending and shear strain energies
T	kinetic energy
u,v,w	displacements in panel co-ordinates
U	total strain energy
U_m, U_b, U_s	membrane, bending and shear strain energies

x,y	panel co-ordinates (x-along the longitudinal and y-along the circumferential directions)
ε_{xx}, ε_{yy}, ε_{xy}	strains
κ_{xx}, κ_{yy}, κ_{xy}	curvatures
v	the Poisson ratio
ρ	mass density
$(\bullet)$	derivative with respect to time